Magnetic field dependence of coherent population transfer by the stimulated Raman transition

R. B. Li,[1,2,3] P. Wang,[1,2,3] H. Yan,[1,2,3] J. Wang,[1,2] and M. S. Zhan[1,2,*]

[1]*State Key Laboratory of Magnetic Resonance and Atomic and Molecular Physics, Wuhan Institute of Physics and Mathematics,*
Chinese Academy of Sciences, Wuhan 430071, China
[2]*Center for Cold Atom Physics, Chinese Academy of Sciences, Wuhan 430071, China*
[3]*Graduate School, Chinese Academy of Sciences, Beijing 100080, China*

Stimulated Raman transition is generally used for a coherent population transfer in a cold atom interferometer. We have experimentally investigated the magnetic field dependence of coherent population transfer by the stimulated Raman process. Experimental data show that both Rabi frequency and population greatly depend on the amplitude and sense of the magnetic field. Theoretical analysis is also carried out, and the experimental results are in good agreement with the theoretical calculations. The study is helpful for optimizing the interferometer fringes and for improving the rotation measurement precision of a Sagnac interferometer.

Since the Raman type atom interferometer using $\frac{\pi}{2} - \pi - \frac{\pi}{2}$ excitation Raman pulse sequence was realized in 1991 [1], its application has been found in the wide field of precise measurement, such as rotation [2,3], gravity acceleration and its gradient [4–6], the fine structure constant α [7], and others [8–10]. The absolute uncertainty of $\Delta g / g = 3 \times 10^{-9}$ has been achieved in the measurement of the gravity acceleration [4]. The atom-interferometer based Sagnac gyroscope of high sensitivity with long-term stability has been reported [11]. Its bias stability is better than 70 μ° / h, and short-term noise is about 3 $\mu^\circ / \sqrt{h}$. To improve the measurement accuracy of the rotation rate of the Earth by using an atom-interferometer based gyroscope, the potential systematic error should be considered and eliminated as much as possible.

The stimulated Raman pulses with large one-photon detuning are used in the atom interferometer. These pulses not only induce the coherent population transfer between two ground states but also transmit two-photon recoil momentum to the atoms. Early studies found that coherent transition probability depends on laser detuning, polarization, Rabi frequency, and interaction time [12–14], but the dependence of population transfer on the magnetic field has not been fully demonstrated. In the interferometer loop area, a weak homogenous magnetic field should be used to avoid energy-level degeneracy and keep the quantum axis consistent. The sense of the magnetic field will affect the Raman-pulse area when the laser polarization is considered. Although atoms are manipulated in $m_F = 0$ sublevel in the atom interferometer, the quadratic Zeeman effect still exists. The systematic error induced by the magnetic field may affect the accuracy of rotation measurement. It is important to systematically investigate the dependence of the stimulated Raman process on the magnetic field.

In this paper, we theoretically analyzed the stimulated Raman process for a Λ-type three level system with an existing magnetic field. We experimentally demonstrated that Rabi frequency depends on the sense of magnetic field. It will help us to strictly define the $\frac{\pi}{2}$ pulse and π pulse, which effectively increase the contrast of atom-interferometer fringes.

We also demonstrated the dependence of population oscillation on the Raman beam intensities and the magnetic field. This provides an experimental criterion of the zero point of the magnetic field in the interferometer area. It will help us to improve the accuracy of the atom-interferometer gyroscope for the rotation measurement by compensating the residual magnetic field to decrease the influence of the quadratic Zeeman effect.

In a Λ-type three-level system as shown in Fig. 1, we consider that E_1 only couples $|a\rangle$ and $|i\rangle$ while E_2 couples $|b\rangle$ and $|i\rangle$ as discussed in the Ref. [15]. Under the rotating-wave approximation and the adiabatic approximation, the intermediate state $|i\rangle$ can be eliminated adiabatically and a Λ-type three-level system is treated as a two-level system with effective Rabi frequency $\Omega_R = \frac{1}{\hbar^2} \langle b | d_2 E_2^* | i \rangle \langle i | d_1 E_1 | a \rangle / 2\Delta$. With the system initially populated in state $|a\rangle$, the population of state $|b\rangle$ after a duration τ is

$$P_b(\tau) = \frac{\Omega_R^2}{\Omega_R^2 + \delta^2} \sin^2 \left(\sqrt{\Omega_R^2 + \delta^2} \frac{\tau}{2} \right), \tag{1}$$

where Δ is the one-photon detuning and δ is the two-photon detuning which includes ac Stark shift and Zeeman shift. The ac Stark shift can be canceled by changing the intensity ratio of the Raman beams [6,16]. The relative quadratic Zeeman shift between $m_F = 0$ and $m_{F'} = 0$ is [17–19]
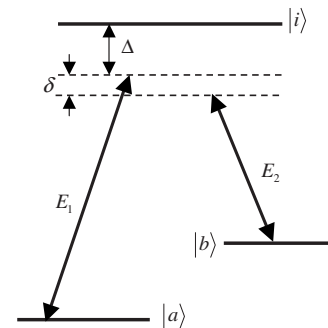

FIG. 1. Level scheme for stimulated Raman transitions with large one-photon detuning. It can be effectively treated as a two-level system.

*mszhan@wipm.ac.cn

$$\delta = \frac{[g_J(S) + g_I']^2 \mu_B^2 B^2}{6h^2 A_S}, \tag{2}$$

where $g_J(S)$ is the electronic g factor, g_I' is the nuclear g factor, μ_B is the Bohr magneton, h is the Planck constant, A_S is the dipole hyperfine constant, B is the magnetic field.

When the light fields are in the standard tensor form $E_1 = \varepsilon_1 \widehat{e_1} + \varepsilon_0 \widehat{e_0} + \varepsilon_{-1} \widehat{e_{-1}}$, $E_2 = \xi_1 \widehat{e_1} + \xi_0 \widehat{e_0} + \xi_{-1} \widehat{e_{-1}}$, the effective Rabi frequency can be written as

$$\Omega_R = \frac{|e|^2}{\hbar^2 2\Delta} \sum_{K=0}^{2} \sum_{Q=-K}^{K} (-1)^Q a_{-Q}^{(K)} \langle b | R_Q^{(K)} | a \rangle \tag{3}$$

with

$$a_{-Q}^{(K)} = \sum_{p,q=-1}^{1} \langle 1q1p | KQ \rangle \varepsilon_{-p} \xi_{-q}, \tag{4}$$

$$R_Q^{(K)} = \sum_{i} \sum_{p,q=-1}^{1} \langle 1q1p | KQ \rangle (r_q | i \rangle \langle i | r_p). \tag{5}$$

From Eqs. (4) and (5), we know that $\langle b | R_Q^{(K)} | a \rangle$ contains only atomic quantities which can be solved by the Wigner-Eckart theorem [20], and $a_{-Q}^{(K)}$ depends on the laser polarizations. We should use a rotating matrix $D_{QQ'}^{(K)}$ when there is an angle β between the Raman beam propagating direction and the magnetic field direction [20–22]. For (σ^+, σ^+) configuration, the polarization tensor components for $Q=0$ are

$$\tilde{a}_0^{(0)} = \frac{1}{\sqrt{3}} \varepsilon \xi, \tag{6}$$

$$\tilde{a}_0^{(1)} = \frac{1}{\sqrt{2}} \cos \beta \varepsilon \xi, \tag{7}$$

$$\tilde{a}_0^{(2)} = -\frac{1}{\sqrt{6}} \left(\frac{3}{2} \sin^2 \beta - 1 \right) \varepsilon \xi, \tag{8}$$

where $\cos \beta = \frac{B}{\sqrt{B^2 + B_0^2}}$, B and B_0 are the magnetic field parallel and perpendicular to the Raman beam propagating direction, respectively. The effective Rabi frequency can be controlled by adjusting the direction of magnetic field as well as the Raman beam intensities, and becomes finally

$$\Omega_R = \frac{|e|^2 \sqrt{I_1 I_2}}{\hbar^2 2\Delta} \sqrt{\frac{\mu_0}{\varepsilon_0}} \sum_{i} \langle b | r_q | i \rangle \langle i | r_p | a \rangle \cos \beta. \tag{9}$$

We only consider $K=1$, $Q=0$ in Eq. (9). Filling Eqs. (2) and (9) into Eq. (1), the population dependence on the magnetic field can be seen obviously. The results are shown in Figs. 5 and 6.

For the ^{85}Rb atoms, hyperfine level $F=2$ is split into five sublevels and $F=3$ into seven sublevels when there exists a magnetic field. The Raman beams can in principle drive all transitions with nonzero transition probability. The best choice, in the three-pulse atom interferometer, is to select the magnetically insensitive transition $|F=2, m_F=0\rangle \rightarrow |F=3, m_F=0\rangle$ to avoid the first order Zeeman shift although the second order Zeeman shift still exists. Only the intermediate states $F'=2, m_{F'}=1$ and $F'=3, m_{F'}=1$ for the (σ^+, σ^+) com-
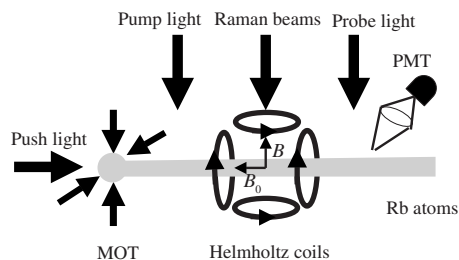

FIG. 2. Experiment scheme: Cold atoms' (^{85}Rb) flight horizontally from the MOT to the probe region. The magnetic field can be adjusted through the currents of two pairs of Helmholtz coils. Laser-induced fluorescence signal is detected by PMT.

bination are involved for the selection rules in the Raman transition, and the loss due to spontaneous emission Γ is ignored because of the large detuning of the Raman beams ($\Delta=1.5$ GHz) in our experiment.

A diagram of the experimental apparatus is shown in Fig. 2. A nonmagnetic stainless steel chamber with 14 windows was used for the magneto-optical trap (MOT). The cooling and trapping light was provided by a tapered amplifier diode laser (TOPTICA TA100) and the repumping laser was from an external-cavity diode laser (TOPTICA DL100). The trapping laser frequency was red-detuned by an amount 2Γ relative to $5S_{1/2}, F=3 \rightarrow 5P_{3/2}, F'=4$ transition and the repumping laser frequency was stabilized to the transition $5S_{1/2}, F=2 \rightarrow 5P_{3/2}, F'=3$. The laser frequencies were locked using the saturated absorption spectroscopy method [23]. The detailed description of the MOT and Raman laser arrangement is similar to our previous work [24]. Briefly, after the polarization gradient cooling (PGC) process, the MOT magnetic field and the trapping light were switched off, and we applied a near resonance laser pulse to push the cold atom cloud fly transversely [25] from the trapping region to the probe region at a velocity of 24 m/s as shown in Fig. 2. Then the flying atoms were completely pumped to the $5S_{1/2}, F=2$ ground state with a perpendicular laser beam near resonance with the transition $5S_{1/2}, F=3 \rightarrow 5P_{3/2}, F'=2$. In the interference area, two pairs of Helmholtz coils control the magnetic field strength of B and B_0, thus the direction, and a pair of Raman beams with circularly polarization is propagating along one of them. The frequency difference of Raman beams is resonant with the ground states transition $F=2, m_F=0 \rightarrow F=3, m_F=0$. Population of one of two ground states $F=2, m_F=0$ or $F=3, m_F=0$ was detected by laser induced fluorescence signal (LIF), and we used a photo multiplier tube (PMT) to collect the LIF.

We have observed Rabi oscillation with different Rabi frequencies for different magnetic field direction while varying the total Raman beam intensity, as shown in Fig. 3. The population oscillates with the Raman beam intensity increased, and the oscillation frequency (Rabi frequency) depends on the magnetic field direction. Here in our experiment, we used a fixed $B=250$ mG parallel magnetic field to the Raman beams, and then gradually increased the perpendicular magnetic field B_0 with a step of 100 mG. The two-photon detuning is zero after the quadratic Zeeman shift is compensated by adjusting the frequency difference of two Raman beams for each of the Rabi oscillation curves, which
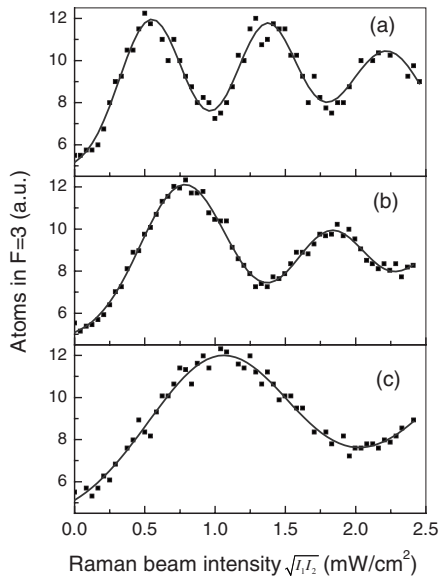
FIG. 3. Rabi oscillation of the stimulated Raman transition. The populations depend on the Raman beam intensities while the periods rely on the direction of the magnetic field. (a), (b), and (c) are typical data for $\beta=0°$, $40°$, and $60°$, respectively. Curves are experimental fits for a Gaussian decay envelope.

is realized by changing the microwave frequency of the acousto-optic modulator (AOM) [24]. Figures 3(a)–3(c) in are Rabi oscillations for $\beta=0°$, $40°$, and $60°$, respectively, where β is the angle between the Raman beams and the resultant magnetic field. The relation between the Rabi frequency and β is shown in Fig. 4, which is consistent with our expectation from Eq. (9).

We have also realized the population transfer and the population oscillations by changing the parallel magnetic field B while maintaining the perpendicular magnetic field B_0 invariable. The experimental results are shown in Figs. 5 and 6. The frequency difference of two Raman beams is fixed at 3 035 732 436 Hz in our experiment, which is resonant with the ground states transition $F=2, m_F=0 \rightarrow F=3, m_F=0$ when the magnetic field does not exist [26]. The laser power of Raman beams is 2.28 mW (the diameter of laser beam is 1 cm) in Fig. 5, and Figs. 5(a)–5(c) correspond to the perpendicular magnetic fields of $B_0=0$, 250, and 500 mG, respec-
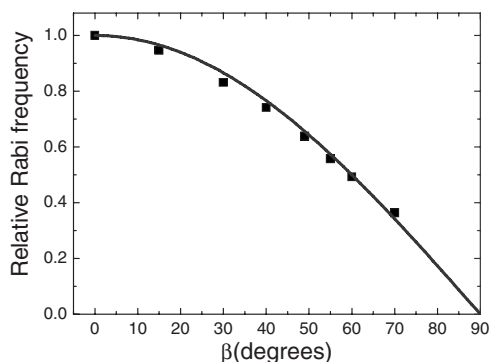

FIG. 4. Dependence of the relative Rabi frequency on the magnetic field direction. The relative Rabi frequency is a cosine function of β, where β is the angle between the Raman beams and the resultant magnetic field.
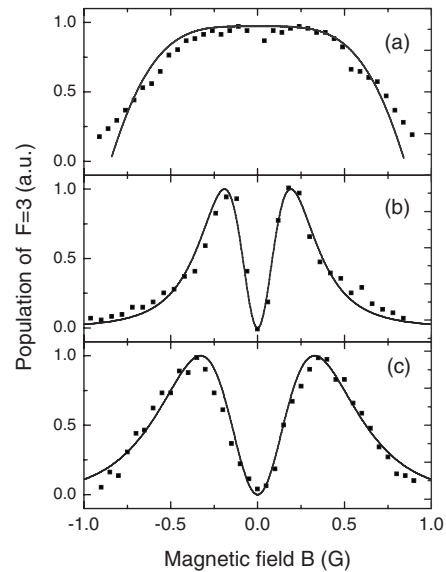

FIG. 5. Population dependence on the magnetic fields B and B_0. Plots (a), (b), and (c) are for $B_0=0$, 250, and 500 mG, respectively. The laser power of Raman beams is 2.28 mW. The solid lines are theoretical results, while the dots are experimental data.

tively, while in Fig. 6, the perpendicular magnetic field is fixed at 500 mG, and plots Figs. 6(a)–6(c) are results corresponding to laser powers of 1.72, 3.21, and 5.16 mW, respectively. The dots are experimental data while the solid lines are theoretical results. Positive and negative magnetic field are for (σ^+, σ^+) transition and (σ^-, σ^-) transition, respectively when the co-propagating direction of the circularly polarized Raman beams are fixed. We can conclude from experimental results that the population distributions of state $F=3$ for the (σ^+, σ^+) pair are the same as for (σ^-, σ^-), which is consistent with the theoretical prediction of the relative

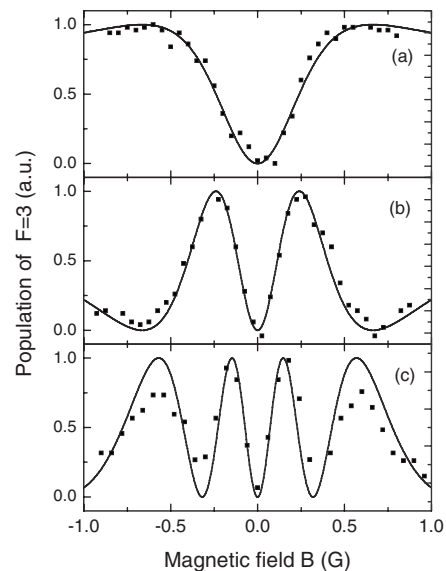
FIG. 6. Population distribution in $F=3$ vs the parallel magnetic field B. The perpendicular magnetic field strength is $B_0=500$ mG, and plots (a), (b), and (c) correspond to laser powers of 1.72, 3.21, and 5.16 mW, respectively. The solid lines are the theoretical prediction, while the dots are experimental data.

transition probability of a two-photon process. The transition impossibly happens when Raman beams are perpendicular to the magnetic field. Two or more peaks emerge for (σ^+, σ^+) or (σ^-, σ^-) when the Raman beam intensity becomes stronger, as shown in Figs. 6(b) and 6(c). The population mainly depends on the two-photon detuning induced by the quadratic Zeeman shift with the parallel magnetic field in Fig. 5(a), which depends on both the two-photon detuning induced by quadratic Zeeman shift with the resultant magnetic field and the sense of magnetic field when the perpendicular magnetic field is applied in Figs. 5(b) and 5(c) and Figs. 6(a)–6(c). This can be well explained when inserting Eqs. (2) and (9) into Eq. (1).

The Sagnac gyroscope based on the atom interferometer is usually realized by the excitation Raman pulses $\frac{\pi}{2}-\pi-\frac{\pi}{2}$ combined with three separated Raman beams [2]. Recently, the new configuration is applied by three single Raman beam pairs pulsed in time to measure three axes of rotation and acceleration in cold atom interferometer [3]. Since the magnetic field distribution of the atom interferometer area inside the magnetic shield is relatively complex [5], the external compensation is necessary to improve measurement accuracy of the Sagnac gyroscope. This work (Figs. 5 and 6) can provide a criterion of zero point of the magnetic field along Raman beams. The residual magnetic field can be canceled completely in the interferometer area by using three Helmholtz coils, and a very small bias magnetic field is applied to keep the quantum axis, which will effectively improve the accuracy of the rotation rate measurement. The contrast of the atom interferometer can be improved when we strictly define the $\frac{\pi}{2}$ pulse and the π pulse after considering the dependence of Rabi frequency on the sense of magnetic field (Figs. 3 and 4). The Raman pulse area is usually determined

by interaction time and effective Rabi frequency. The larger intensity and longer interaction time is needed to obtain the same Raman pulse area when the perpendicular magnetic field exists. In the experiment, the atoms with different velocity distribution interact with different positions in the Gaussian Raman intensity envelope. The variation of the Rabi frequency of the atomic cloud makes the Rabi oscillation damped, as shown in Fig. 3. This means that the coherence is broken slightly when the Raman beam intensity and the interaction time are increased [5], which makes the contrast of atom interferometer decrease. The Raman beam intensity and the interaction time should be as small as possible for the π pulse and the $\frac{\pi}{2}$ pulse after the perpendicular magnetic field is canceled completely. In addition, the perpendicular magnetic field will increase the quadratic Zeeman shift, and the accuracy of the Sagnac gyroscope will be influenced.

In summary, we have experimentally studied the coherent population transfer induced by a stimulated Raman process and its dependence on the magnetic field. We demonstrated that the population varies with the strength and sense of the magnetic field. The frequency of Rabi oscillation is a cosine function of the angle between the magnetic field and the Raman beams. The results will help us to improve the contrast of the atom-interferometer fringes and the accuracy of the measurement of rotation using $\frac{\pi}{2}-\pi-\frac{\pi}{2}$ configuration in future atom-interferometer Sagnac gyroscopes.

[1] M. Kasevich and S. Chu, Phys. Rev. Lett. **67**, 181 (1991).
[2] T. L. Gustavson, A. Landragin, and M. Kasevich, Class. Quantum Grav. **17**, 2385 (2000).
[3] B. Canuel, F. Leduc, D. Holleville, A. Gauguet, J. Fils, A. Virdis, A. Clairon, N. Dimarcq, C. J. Borde, A. Landragin, and P. Bouyer, Phys. Rev. Lett. **97**, 010402 (2006).
[4] A. Peters, K. Y. Chung, and S. Chu, Nature (London) **440**, 849 (1999).
[5] A. Peters, Ph.D. thesis, Stanford University, Palo Alto, CA.
[6] T. Petelsk, Ph.D. thesis, University of Florence, Florence.
[7] D. S. Weiss, B. C. Young, and S. Chu, Phys. Rev. Lett. **70**, 2706 (1993).
[8] A. Morinaga, T. Aoki, and M. Yasuhara, Phys. Rev. A **71**, 054101 (2005).
[9] C. L. Webb, R. M. Godun, G. S. Summy, M. K. Oberthaler, P. D. Featonby, C. J. Foot, and K. Burnett, Phys. Rev. A **60**, R1783 (1999).
[10] C. R. Hagen, Phys. Rev. Lett. **64**, 2347 (1990).
[11] D. S. Durfee, Y. K. Shaham, and M. A. Kasevich, Phys. Rev. Lett. **97**, 240801 (2006).
[12] B. W. Shore, J. Martin, M. P. Fewell, and K. Bergmann, Phys. Rev. A **52**, 566 (1995).
[13] J. Martin, B. W. Shore, and K. Bergmann, Phys. Rev. A **52**, 583 (1995).
[14] J. Martin, B. W. Shore, and K. Bergmann, Phys. Rev. A **54**, 1556 (1996).
[15] K. Moler, D. S. Weiss, M. Kasevich, and S. Chu, Phys. Rev. A **45**, 342 (1992).
[16] R. W. Schmieder, Am. J. Phys. **40**, 297 (1972).
[17] W. M. Itano, J. Res. Natl. Inst. Stand. Technol. **105**, 829 (2000).
[18] G. P. Barwood, K. Gao, P. Gill, G. Huang, and H. A. Klein, Phys. Rev. A **67**, 013402 (2003).
[19] M. Kajita, Y. Li, K. Matsubara, K. Hayasaka, and M. Hosokawa, Phys. Rev. A **72**, 043404 (2005).
[20] I. I. Sobelman, *Atomic Spectra and Radiative Transitions* (Springer, New York, 1996), p. 61.
[21] R. Wynands, A. Nagel, S. Brandt, D. Meschede, and A. Weis, Phys. Rev. A **58**, 196 (1998).
[22] L. C. Biedenharn and J. D. Louck, *Angular Momentum in Quantum Physics* (Addison-Wesley, Reading, MA, 1981), p. 46.
[23] J. Wang, X. J. Liu, J. M. Li, K. J. Jiang, and M. S. Zhan, Chin. J. Quantum Electronics **17**, 44 (2000).
[24] P. Wang, R. B. Li, H. Yan, J. Wang, and M. S. Zhan, Chin. Phys. Lett. **24**, 27 (2007).
[25] K. J. Jiang, K. Li, J. Wang, and M. S. Zhan, Chin. Phys. Lett. **22**, 324 (2005).
[26] S. Penselin, T. Moran, and V. W. Cohen, Phys. Rev. **127**, 524 (1962).